Dear Editor, Dear reviewers,

Thank you for dedicating your time to review our work. We have replied in our Author Response below to ‘Review’ in RC1 and ‘Review’ in RC2. This document ends with the marked-up manuscript, showing the changes we have made to the original version. Besides these files, a new version of the dataset is now available at https://doi.org/10.11582/2019.00019.

Yours sincerely,

Anne Morée and Jörg Schwinger

Author Comment to 'Review' in RC1

1. Explain the use of the *.md5 files

*The *.md5 files contain an md5 checksum, which can be used to check whether changes have been made to the respective *.nc files. The md5 checksum of the .nc files should thus be identical to the ones in the *.md5 files. Such checks can be done with several freely available online tools.*

Changes made in the manuscript: An explanation is provided in Sect. 4 on Data Availability.

2. Comment on the novelty of the dataset

The reviewer is of course right that the PMIP model results underlying our dataset are publicly available, and that everyone could go to the PMIP archives and repeat our efforts. The assertion that this could be done "very straightforwardly", however, underestimates the amount of work put into the compilation of this dataset considerably. There has been a long series of decisions and considerations involved, starting from compiling data availability across variables and models, to scientific questions of how to treat differences in topography and land-sea mask, and how to re-reference the temperature and humidity fields. The authors expect that the availability of i) a direct visual impression of PI-LGM PMIP3 anomalies and model spread, ii) the clear description of the concept (f.e., CDO/NCO procedure and the idea of anomaly addition to original forcing) and iii) the freely available download of the relevant variables in one standard format will be valuable for future LGM modeling attempts. Indeed, the authors have already received interest from several colleagues about the dataset. Moreover, users inexperienced with PMIP/CMIP/CDO/NCO now have a clear presentation of this opportunity in LGM modeling, which increases the likelihood of modeling attempts by such users. Also, models for which a fully coupled LGM run is not (yet) available, or models that are inherently ocean-only, now have a relatively accessible way to simulate the LGM without needing to prepare such forcing datasets themselves.

Changes made in the manuscript: None

3. How does one estimate NY (intra-annual) forcing typical of G-IG anomaly?

The construction of a "normal year" forcing (NYF) is indeed not trivial. Large and Yeager (2004; http://opensky.ucar.edu/islandora/object/technotes:434) describe their procedure for the CORE NYF in detail. However, our objective is not to construct a LGM normal year forcing in a strict sense, but to provide LGM-PI anomaly fields that can be used in combination with the existing CORE (and other) forcing fields. If added to the CORE NYF one obtains a LGM "normal year" forcing under the assumption that –beyond changes in the monthly mean state– the temporal and spatial statistics of the forcing fields are the same under LGM conditions. We see that this assumption was not made explicit in our manuscript, and we propose to add text to clarify that we focus on CORE forcing formats, and that the use of an anomaly dataset implies certain assumptions.

Changes made in the manuscript: We added additional text in the abstract and Sect. 2 to clarify our intensions (optimized presentation for use with CORE forcing) and assumptions (unchanged spatial and time variability).

4. How should we handle the range of inter-model spreads?

The authors address how to use the model spread at the end of the manuscript: '..., all mean anomalies show a distinct spatial pattern that we expect to be indicative of the LGM-PI changes. […]. For modelling purposes, the inter-model disagreement of PMIP3 provides the user with leeway to adjust the amplitude of the forcing (within the model spread). Such adjustments can improve model-proxy data agreements, such as described for salinity in Sect. 3.7.' Moreover, such adjustments, or 'tuning', of an ocean-only model could inform fully coupled models by revealing model sensitivities. A good example of this is SSS, for which the PI-LGM anomaly is likely too large in the North Atlantic for most PMIP models, pointing to a potential limitation in hydrological cycling of these models (Sect. 3.7).' We acknowledge that we do not know how to objectively handle model spread beyond using it to "justify" model tuning – but think that a discussion of PMIP3 model spread is beyond the scope of the article (p. 6, l. 24-25). The user is provided with the model spread for each variable in a new version of the dataset, in order to improve the usability of the model spreads (see also comment 7).

Changes made in the manuscript: Sect. 2 now includes two sentences describing the availability of the model spread alongside the forcing anomaly fields, and what we expect it can be used for. The caption of Table 1 has also been extended to clarify this. We made a new version of the dataset (version 2) that includes the model spread (https://doi.org/10.11582/2019.00019).

5. How can we include information from available observations?

We believe that for most atmospheric variables (e.g., wind, humidity, radiation), global coverage through LGM proxy data will be never achieved. For model forcing we thus have to rely on model simulations of the variables of interest. Comparison of model results to proxy data that are available (such as estimates of AMOC strength, sea ice extent or productivity for example) is a useful tool for model evaluation (Braconnot et al., 2012). For some atmospheric variables however (e.g., air temperature) one could use proxy data to guide corrections to the model mean anomaly (in addition to the model spread). We leave it to the individual modeling groups to adjust the mean anomalies if considered necessary/needed for their purposes. We extended the text with information on how the authors think observational/proxy estimates can best be used.

Changes made in the manuscript: We extended Sect. 2 with a comment on proxy data as a potential anomaly constraint together with the model spreads.

6. Why are some fields interpolated to 6-hourly and others to daily fields?

Our intention is to provide the data in CORE forcing format (p. 3, l. 15-16), which could be either NY or interannually varying CORE forcing. For the variables specific humidity, wind components and air temperature CORE forcing is based on the NCEP-reanalysis, which has a standard time resolution of 6 hours (Large and Yeager, 2004). For radiation fluxes, daily is the highest time resolution in the CORE forcing (Large and Yeager, 2004), and therefore used in our dataset. Similarly, for precipitation and SSS, we conform to the CORE forcing standard (monthly time resolution; Large and Yeager, 2004). We made this clearer in the manuscript by extending the caption of Table 1, and stressing our focus on the CORE format earlier in the manuscript/abstract.

Changes made in the manuscript: The caption of Table 1 and the text in Sect. 2 and the abstract are extended to stress our intension to provide CORE format data (see also our reply to comment 3).

7. While model spread is plotted in the figures, I could not locate this as a variable in the data.

We understand this can be a valuable additional variable for the potential user, and added it to the dataset for all variables named 'variablename_spread'.

Changes made in the manuscript: No changes were made in the manuscript, but a new version of the dataset (version 2) was made (https://doi.org/10.11582/2019.00019) that included the model spread for each variable (with name variable_spread).

8. There may be some grid-scale interpolation artifacts along coastlines (Fig. 1)

The most pronounced changes in humidity occur along the coastlines. This is not an artifact of the time or vertical interpolation, but a consequence of the different lgm land-sea mask as compared to the piControl land-sea mask. As some ocean becomes land along most coastlines, a local reduction occurs there in specific humidity.
We realize that this is suboptimal, although it is only clearly visible for specific humidity and not relevant for groups that would apply an lgm land-sea mask. However, we want the files to be of use for modeling groups that want to use a pre-industrial land-sea mask as well (e.g. for idealized experiments). To remedy this inconsistency we propose the following approach:
1) Mask the multi-model mean anomaly as we present it now by the maximum lgm land area across all models,
2) Extrapolate variables over land using a distance-weighted average,
3) Mask the data with a decreased present-day land mask (decreased such that we insure that any pre-industrial land-sea mask is covered by the anomaly for all its ocean grid cells).
The area affected by land-sea mask changes is thus filled with the extrapolated model mean anomaly. Coastal effects under the area affected by a changing land-sea mask are thus removed for all variables. We note that the extrapolatation over the large Arctic continental shelves (which are land during the lgm model runs, and sea during the piControl model runs) leads to artificial structures in the specific humidity anomaly field (top figure). These structures are only relevant if a user applies a present-day land-sea mask, and - we expect - will not cause any problems as the anomaly gradients are similar to those in other regions (f.e. the North Pacific). In addition, no topography correction is now needed for surface temperature, as the field is now only based on open-ocean model data. We tested this approach in NorESM-OC, and see no problems with the initialization caused by the masking.

Changes made in the manuscript: Sect. 2 now includes an explanation of the masking. In the new version of our dataset (version 2), we provide all atmospheric fields with a decreased pre-industrial land mask where the anomaly is set to zero. We include the maximum lgm and decreased 'pre-industrial' masks in each data file such that the user can readily see which part of the data are extrapolated values.

9. The salinity fields look strange and unlike the figure in the manuscript (Fig. 2) (unless I'm doing something wrong to access the file; I used ncread('Salinity_anomaly_1deg.nc','sos',[1,1,4],[360,180,1]); in MATLAB).

The salinity field is the only field provided on a 1x1 degree grid. The field was provided for all grid-cells (extrapolated over land) such that it can be used with any land-ocean mask, as described in the text

(Sect. 3.7). As this causes confusion, we now provide the data in masked form (see our answer to comment 8).

Changes made in the manuscript: We removed the extrapolation procedure from Sect. 3.7 as this is now explained for all variables in Sect. 2. In the new version of the dataset (version 2), no smoothing is needed anymore for sea surface salinity (as we now use more models, see our reply to the other reviewer), so this is also removed from the text.

10. Please say what NCO is

NetCDF Operators (NCO) is a NetCDF toolkit (http://nco.sourceforge.net/#Definition) that can be used besides or in addition to CDO.

Changes made in the manuscript: At the introduction of CDO and NCO in Sect. 2, we now clarify that each of these are toolkits to handle NetCDF data.

11. There are several thorny issues associated with forcing a model with multi-model means. For one, the fields are no longer dynamically consistent. An implication is that there could be strangely conflicting contributions e.g. to surface salinity from relaxation and precipitation. Second, have these models all been run to equilibrium? Third, computing ensemble means tends to damp uncorrelated variability between members, which reduces the variance of forcing fields. Is there a way to correct for this and generate a "normal year"?

i-a) Dynamic consistency: The CORE forcing itself is not dynamically consistent, since it is a blend of different sources (NCEP reanalysis, satellite and surface observations). This is apparently not seen as a major problem in the ocean modelling community (the CORE forcing is widely used, e.g. recently in CMIP6-OMIP). We are not aware either of any study investigating such dynamical inconsistencies in the context of ocean modeling. From this standpoint, we believe that the inconsistencies that are introduced by using a multi-model mean for our anomaly forcing are not a major issue.

i-b) Salinity relaxation and precipitation: Freshwater balance and salinity relaxation need special attention for multi-centennial forced ocean model simulations. Using the CORE forcing, precipitation is prescribed but evaporation and SSS evolve freely such that imbalances can and will develop. Groups applying the CORE forcing (and our anomaly forcing) will be able to deal with such complications (e.g. enforce freshwater balance globally by adjusting precipitation, balance salinity relaxation to conserve total salinity). In NorESM-OC, this is for example done by enforcing global freshwater-flux balance (by adjusting precipitation with a global correction factor). Also, salinity relaxation is applied such that the global net flux of salt into the surface ocean is zero. Again, these issues occur already when the original CORE forcing is used and are not specific to our anomaly forcing.

ii) Equilibrium: CMIP/PMIP models have been run to equilibrium as much as feasibly possible considering the high costs of computing. The authors comment on this in lines 1-6, p. 2. The output of the different CMIP/PMIP model experiments is considered a reasonable estimate of the past global climate state – which is required for our use. We expect that issues with persistent model drift more likely would arise for interior/deep ocean model fields. Nevertheless, we do acknowledge, that part of the inter-model spread may be explained by differences in the extent to which the respective PMIP model has approached equilibrium. As we comment on equilibration already in l. 1-6 on p. 2, we think no further action is required.

iii) Damped uncorrelated variability: We agree with the reviewer that this is an issue with our multi model approach that is not mentioned in our manuscript. The preferred method of using an ensemble of N fully coupled models to force a standalone ocean model would be to create an ensemble of N forcings and run the standalone model for each of the forcings separately. Of course, the drawback of this approach is the N-fold increase in computational resources (cpu and storage). We believe that for the sake of achieving long integrations of the LGM ocean state, it is justifiable to use a multi model mean anomaly. In addition, the anomalies are generally small (< 10 %) as compared to the forcing field. We see that it would be good to mention these considerations explicitly in our manuscript.

In general, we acknowledge that it is important to mention the sources of error coming from the use of multi-model means.

Changes made in the manuscript: Sect. 2 has been extended to include a comment on dynamical inconsistencies and dampening of uncorrelated variability.

12. Are effects of evaporation included in the precipitation file?

The variable 'pr' presented in the dataset represents the total amount of precipitation (liquid and solid phases, and from all types of clouds – both large-scale and convective)). Evaporation is thus not included in the precipitation fluxes, and should be calculated by the model itself based on evaporative forcing (through f.e. temperature and humidity).

Changes made in the manuscript: We made it explicit in Sect. 3.4 that the precipitation anomaly excludes evaporation.

13. It would be helpful to provide a river runoff file.

The authors found that the CMIP river runoff variable (friver, 'Water Flux into Sea Water From Rivers (kg m-2 s-1)') is only available for CNRM-CM5, IPSL-CM5A-LR, MIROC-ESM and MRI-CGCM3 for the lgm. Besides that, the differences in land-sea masks of these models are problematic as river outlets may end up off-coast or on land when applied in a forced ocean model. Averaging over such 'point-sources' will create a little meaningful product in our opinion, as the river outlets vary considerably between models. In NorESM-OC, we route the preindustrial river runoff to the nearest ocean grid-cell, but such solutions are very model dependent, and we expect that modelling groups devise a suitable solution for their specific model for the treatment of runoff.

Changes made in the manuscript: We extended Sect. 3.4 with a comment on river runoff and our recommendations to follow PMIP guidelines.

14. Sect. 3.6 line 10 'due to' changes?

'due to' is indeed missing here. Thank you for noting this mistake.

Changes made in the manuscript: None - as the topography-corrected temperature anomaly is not provided in version 2 of our dataset due to the masking and extrapolation procedure (see our reply to comment 8), this sentence is not present in the manuscript anymore.

Author Comment to 'Review' in RC2

General Comments

1. Improvable Data References:

References for the source data should be added. As part of the terms of use for CMIP5 data, apart from the existing acknowledgement, data collections should be referenced in the article's body and cited in the reference list. For CMIP5 references could be found on the IPCC DDC web page for the AR5 Reference Data Archive: http://www.ipcc-data.org/sim/gcm_monthly/AR5/Reference-Archive.html

Thank you for making us aware of more specific references that we could use to acknowledge the modeling groups and their specific experiments.

Changes made in the manuscript: We extended Table 2 to include the experiment specific references and updated the reference list accordingly.

2. Improvable provenance information:

CMIP5 datasets used should be specified using the full DRS (Data Reference Syntax) including their versions and tracking_ids. All additionally needed datasets like 'psl' and 'ts' (p.3 l. 30) should be specified. An additional table is suggested.

It would indeed be good to complement the dataset with the original 'version_history' and 'tracking_id' global attributes of each of the models for both the lgm and piControl experiments. The CMIP variables 'psl' and 'ts' were used for the re-referencing to 10m height.

Changes made in the manuscript: In the new version of the dataset (version 2), all variables now have the tracking_id numbers for each of the piControl and lgm output files, as well as the version_history in their global attributes. We specified the names 'psl' and 'ts' in Sect. 3.1, such that it is clear which CMIP variables were used for the re-referencing from 2 to 10 meters.

3. Question: Why did the authors not use the 3D CMIP5 datasets?

The authors state that only the selected four models provided all the required variables. Could the authors explain why they did not use the 3D fields of the model output but based their study on the interpolated (post-processed) surface variables? The 3D fields were provided by more modeling centers. As the authors apply a vertical interpolation to 10 m height for some variables, the direct model output seems to be better suited as source data. Moreover, the number of models could be increased, on which the data is based. These 3D variables are e.g. 'ta' instead of 'tas', 'hus' ('huss') or 'so' ('sos'). Especially the sea surface salinity anomaly, which is currently based on only two CMIP5 datasets (p.5 ll. 24/25), will be more reliable.

The atmospheric 3D fields of CMIP/PMIP are provided on pressure levels. The geopotential height corresponding to the atmospheric pressure level closest to the earth's surface (the 1000 hPa pressure level) is generally ~150-200m above the ocean (CMIP variable 'zg'). The use of the 3D fields on the level of the air-sea interface would thus mean an extrapolation over many tens of meters height for all of the atmospheric variables in our dataset. We expect that the native 2 and 10 meter fields calculated by

each model (internally consistent) will provide a better approximation of the near-surface state. The re-referencing of temperature and specific humidity to 10 m done by us is a minor correction compared to this. The choice of surface fields indeed forces us to reduce the number of models we can base our data on. We noticed however that we can add the GISS-E2-R model (which was left out before because we selected r1i1p1 ensembles only) to our dataset.

For sea surface salinity, the use of the ocean 3D field would indeed be an improvement. It would make it possible to use four of the five atmospheric models (namely CNRM-CM5, GISS-E2-R, MIROC-ESM and MRI-CGCM3). We decided in addition to calculate the monthly climatological sea surface salinity based based on the 'mon' 3D salinity (so) output for IPSL-CM5A-LR, as we have not found the 'monClim' IPSL-CM5A-LR data for piControl variable 'so'.

Changes made in the manuscript: We clarify that the new dataset is based on five models for all variables (Sect. 2). The dataset has been updated (https://doi.org/10.11582/2019.00019), i.e. version 2) to include the GISS-E2-R model for all atmospheric variables. Sea surface salinity is now calculated based on the 3D variable 'so' from PMIP3 (and we updated Table 1 accordingly). The whole dataset is therefore based on the same five models in version 2 of the dataset.

4. Reuse of the data:

As the paper on the 'CORE forcing fields' is cited as reference for the usefulness of the chosen spatial-temporal resolution of the provided datasets for common ocean-only model runs, it should be made accessible (e.g. on Zenodo) if possible. Alternatively, have the authors used the datasets for the forcing of a second ocean-only model run to show the reusability of the dataset, yet?

The Large and Yeager (2004) report is publicly available at the NCAR/UCAR "OpenSky"-repository: (http://opensky.ucar.edu/islandora/object/technotes:434). Experiments with different versions of the CORE forcing data have been done by many modelling groups before – see for example Griffies et al. (2009). The CORE forcing is also used for the Ocean Model Intercomparison Project (OMIP) within CMIP6 (Griffies et al., 2015).

Changes made in the manuscript: We added the DOI url to the report to the Large and Yeager (2004) reference.

5. Further reuse of the data:

The authors state that data users could adjust the data using the spread of the CMIP5 model results (p. 6 ll. 29-31). Then the authors need to provide this information in their data.

We understand this can be a valuable additional variable for the potential user.

Changes made in the manuscript: See also our reply to comment 8 of the other reviewer: We elaborate on the model spread in Sect. 2. The new version of the dataset (i.e., version 2) contains the model spread for each variable alongside the anomaly.

Specific comments

6. Please delete 'CMIP-type' as additional characterization of complex fully coupled models, as it is unclear what that means and it does not add information.

Thank you for noting this.

Changes made in the manuscript: We removed this wording in the Introduction.

7. Data files do not contain any history of the applied commands. cdo writes information on the applied commands into the global attribute 'history'. This provides useful information about dataset creation. Why is that not in the file?

The authors wanted to provide clean files to the user alongside the detailed procedure description in the manuscript. As the reviewer points out, the exact procedure is indeed saved in the history (by both CDO and NCO) and could be useful for the potential user. We will keep the full history off all files as well as their appended file history as a global attribute in an updated version of the dataset.

Changes made in the manuscript: None. However, the new version of the dataset (i.e., version 2) now contains a full history of the CDO and NCO commands used.

8. Data files could include more information not only on the above-mentioned history but also on the methodology. I suggest, the authors add the data doi as a reference to the global attributes, which leads the data user to the doi page with further information.

As the NIRD Research Data Archive does not allow reservation of DOI's, we cannot know before publishing the dataset online what the DOI of the dataset will be. However, we are able to refer to the previous version and state that the user should check for newer versions of the dataset. Similarly, we cannot know the final DOI of an ESSD article, so we can only refer to the ESSDD article.

Changes made in the manuscript: We added a global attribute 'references' with the ESSDD manuscript DOI and the NIRD Research Data Archive dataset DOI (dataset version 1, as we cannot know the new DOI before publication in the archive) and a note to check for updates.

9. Why was the unit of precipitation_flux changed from the NetCDF/CF recommended and within CMIP5/PMIP3 used kg m-2 s-1 to mm/day? The unit should not be changed if not required.

The 1979-2000 GXGXS Precipitation Climatology employed for the CORE forcing is in mm/d (Large and Yeager, 2004), and the authors wish to present a dataset that can be easily used in combination with a models' original CORE forcing.

Changes made in the manuscript: The deviation from the CF-1.6 convention is noted in Sect. 3.4. The conversion factor is provided in the global attribute 'Conventions' in the new version of the dataset.

10. The provided datasets same as the CMIP5 datasets should comply with the NetCDF/CF conventions. This seems to be the case, though I did not check it. Then the version of the convention should be specified in the global attributes as described at: http://cfconventions.org/Data/cf-conventions/cf-conventions-1.7/cf-conventions.html.

We used one of the available online CF compliance checkers to make sure that the dataset follows NetCDF/CF conventions. Note that the units of precipitation do not follow the convention, in order to follow the CORE format convention (see our reply to comment 9).

Changes made in the manuscript: We added the version of the convention (CF-1.6) as a global attribute in the new version of the dataset.

11. The authors should add a sentence on the relation of PMIP3 and CMIP5 (PMIP4 and CMIP6 resp.) for readers less familiar with these large intercomparison projects.

We see the need to further clarify the PMIP3-CMIP5 connection in the introduction of the manuscript.

Changes made in the manuscript: We added a sentence in the Introduction explaining what PMIP3 is as part of CMIP5.

12. Is there a reason why the current version 1.9.7 of the cdo package was not used but the old version 1.7.0? Moreover, on the cdo's page 1.7.0 cannot be downloaded (https://code.mpimet.mpg.de/projects/cdo/files). The authors should consider using the current or a more recent version of the cdos.

The somewhat older 1.7.0 version of CDO gives to our knowledge no different results than later versions for the functions we applied to make our dataset. We however see that the use of the most up-to-date version of CDO is desirable, and we are able to use CDO version 1.9.3 on our systems to remake the dataset. We did a test, and see no differences in the result when using 1.9.3 as compared to version 1.7.0.

Changes made in the manuscript: CDO version 1.9.3 and NCO version 4.6.9 were used to make version 2 of the dataset, and noted as a global attributes in the dataset. The text (caption Table 3 and Sect. 2) is updated accordingly.

Technical Corrections

13. CMIP stands for *Coupled* Model Intercomparison Project.

Thank you for noting this mistake.

Changes made in the manuscript: We corrected it in the Introduction of the manuscript.

14. 'lgm' and 'piControl' are the CMIP5 experiment acronyms. It is confusing and unnecessary to introduce the additional acronyms 'LGM' and 'PI' for them.

We chose to use LGM and PI for readability, but decided to change this as it causes confusion.

Changes made in the manuscript: We removed these PI and LGM acronyms from the manuscript wherever they were directly referring to the 'lgm' and 'piControl' PMIP/CMIP experiments.

References

Griffies, S. M., A. Biastoch, C. Böning, F. Bryan, G. Danabasoglu, E. P. Chassignet, M. H. England, R. Gerdes, H. Haak, R. W. Hallberg, W. Hazeleger, J. Jungclaus, W. G. Large, G. Madec, A. Pirani, B. L. Samuels, M. Scheinert, A. Sen Gupta, C. A. Severijns, H. L. Simmons, A. M. Treguier, M. Winton, S. Yeager and J. Yin, 2009: Coordinated Ocean-ice Reference Experiments (COREs). Ocean Modelling, 26, 1–46.

Griffies, S. M., Danabasoglu, G., Durack, P. J., Adcroft, A. J., Balaji, V., Böning, C. W., Chassignet, E. P., Curchitser, E., Deshayes, J., Drange, H., Fox-Kemper, B., Gleckler, P. J., Gregory, J. M., Haak, H., Hallberg, R. W., Heimbach, P., Hewitt, H. T., Holland, D. M., Ilyina, T., Jungclaus, J. H., Komuro, Y., Krasting, J. P.,

Large, W. G., Marsland, S. J., Masina, S., McDougall, T. J., Nurser, A. J. G., Orr, J. C., Pirani, A., Qiao, F., Stouffer, R. J., Taylor, K. E., Treguier, A. M., Tsujino, H., Uotila, P., Valdivieso, M., Wang, Q., Winton, M., and Yeager, S. G.: OMIP contribution to CMIP6: experimental and diagnostic protocol for the physical component of the Ocean Model Intercomparison Project, Geosci. Model Dev., 9, 3231-3296, https://doi.org/10.5194/gmd-9-3231-2016, 2016.

A Last Glacial Maximum forcing dataset for ocean modelling

Anne L. Morée[1], Jörg Schwinger[2]

[1]Geophysical Institute, University of Bergen and Bjerknes Centre for Climate Research, Bergen, 5007, Norway
[2]NORCE Climate, Bjerknes Centre for Climate Research, 5007 Bergen, Norway

Correspondence to: Anne L. Morée (anne.moree@uib.no)

Abstract. Model simulations of the Last Glacial Maximum (LGM, ~21 000 years before present) can aid the interpretation of proxy records, help to gain an improved mechanistic understanding of the LGM climate system and are valuable for the evaluation of model performance in a different climate state. Ocean-ice only model configurations forced by prescribed atmospheric data (referred to as "forced ocean models") drastically reduce the computational cost of paleoclimate modelling as compared to fully coupled model frameworks. While feedbacks between the atmosphere and ocean-sea-ice compartments of the Earth system are not present in such model configurations, many scientific questions can be addressed with models of this type. The data presented here are derived from fully coupled paleoclimate simulations of the Palaeoclimate Modelling Intercomparison Project (PMIP3). The data are publicly accessible at the NIRD Research Data Archive at https://doi.org/10.11582/2019.00019~~https://doi.org/10.11582/2019.00011~~ (Morée and Schwinger, 2019). They consist of 2-D anomaly forcing fields suitable for use in ocean models that employ a bulk forcing approach and are optimized for use with CORE forcing fields. The data include specific humidity, downwelling longwave and shortwave radiation, precipitation, wind (v and u components), temperature and sea surface salinity (SSS). All fields are provided as climatological mean anomalies between LGM and pre-industrial times. These anomaly data can therefore be added to any pre-industrial ocean forcing data set in order to obtain forcing fields representative of LGM conditions as simulated by PMIP3 models. These forcing data provide a means to simulate the LGM in a computationally efficient way, while still taking advantage of the complexity of fully coupled model set-ups. Furthermore, the dataset can be easily updated to reflect results from upcoming and future paleo model intercomparison activities.

1 Introduction

The LGM (~21 kya) is of interest to the climate research community because of the relative abundance of proxy data, and because it is the most recent profoundly different climatic state of our planet. For these reasons, the LGM is extensively studied in modelling frameworks (Menviel et al., 2017; Brady et al., 2012; Otto-Bliesner et al., 2007). Model simulations of the past ocean can not only provide a method to gain a mechanistic understanding of marine proxy records, they can also inform us about model performance in a different climatic state of the Earth system (Braconnot et al., 2012). Typical state-of-the-art tools to simulate the (past) Earth system are climate or Earth system models as, for example, used in the ~~Climate~~ Coupled Model Intercomparison Project phase 5 (CMIP5; Taylor et al. (2011)). Besides simulating our present climate, these CMIP5 models are also used to simulate past climate states (such as the LGM) in the Palaeoclimate Modelling Intercomparison Project 3 (PMIP3).

However, ~~Unfortunately, t~~the computational costs and run-time of such fully coupled model frameworks are a major obstacle for their application to palaeoclimate modelling. Palaeoclimate modelling optimally requires long (thousands to ten thousands of years) simulations in order to provide the necessary time for relevant processes to emerge (e.g. CaCO3 compensation) (Braconnot et al., 2007). Complex ~~CMIP-type~~ fully coupled models can typically not be run into full equilibrium (which requires hundreds to thousands of years of integration) due to computational costs (Eyring et al., 2016). Therefore, the~~se~~ PMIP3 models exhibit model drift (especially in the deep ocean, e.g. Marzocchi and Jansen (2017)). The 3rd phase of the PMIP project (PMIP3; Braconnot et al. (2012)) limits global mean sea-surface temperature drift to under 0.05 K per century and requires the Atlantic Meridional Overturning Circulation to be stable (Kageyama et al., 2018).

The use of PMIP output as ocean forcing is an accepted practice in ocean modelling (e.g., Muglia and Schmittner (2015)). We refer to a "forced ocean model" as a model of the ocean-sea-ice-atmosphere system in which the atmosphere is represented by prescribed 2-D forcing fields. It can be used whenever ocean-atmosphere feedbacks are of minor importance and has the advantage of reducing the computational costs – making longer or more model runs feasible. We present 2-D (surface) anomaly fields ~~(~~of CMIP5/PMIP3 experiments 'lgm'~~LGM~~ minus 'piControl'~~pre industrial)~~ calculated from monthly climatological PMIP3 output. The PMIP3 output is the result of global boundary conditions and forcings (such as insolation and ice sheet cover) applied in the fully coupled PMIP3 models (Braconnot et al., 2012). Our dataset (Morée and Schwinger, 2019) is a unique compilation of existing data, processed and reformatted such that it can be readily applied in a forced ocean model framework that uses a bulk forcing approach similar to Large and Yeager (2004). Since this approach has been popularized through coordinated model intercomparison activities (Griffies et al., 2009), a majority of forced ocean models today uses this approach. The 2-D anomaly fields presented here can be added to the pre-industrial forcing of a forced ocean model in order to obtain an atmospheric forcing representative of the LGM. The data are climatological mean anomalies, and as such suitable for equilibrium LGM 'time-slice' modelling of the ocean. The description of the procedure followed to make this dataset (Sect. 3~~, Table 3~~) should support any extension of the dataset with additional (PMIP-derived) variables if needed. The PMIP4 guidelines (Kageyama et al., 2017) can support users in designing a specific model set-up, for example regarding the land-sea mask, trace gas concentrations, river ~~outflow~~ runoff or other conditions and forcing one would want to apply to a model. In Sect. 2, a general description of the dataset and data sources is provided alongside with an overview of the variables (Table 1).

2 General description of the dataset

The data presented in this article are 2-D anomaly fields of the LGM versus pre-industrial state (experiment 'lgm' minus experiment 'piControl'~~LGM minus pre industrial~~) based on the PMIP3 (Braconnot et al., 2012). These anomaly fields can be used as atmospheric LGM forcing fields for ocean-only model set-ups when added to pre-industrial forcing fields, and are optimized for use in combination with Coordinated Ocean-ice Reference Experiments (CORE) forcing fields (Griffies et al., 2009). The use of an anomaly forcing implies the assumption that no changes in temporal or spatial variability occurred between the lgm and piControl states beyond changes in the mean. We note that by adding multi model mean anomalies to forcing fields, dynamical inconsistencies (e.g. between wind and temperature fields) could be created. A forcing data set would typically be dynamically

consistent if the forcing would be the outcome of an advanced atmospheric reanalysis. However, the CORE forcing is a mixture of reanalysis and observational data products, and we assume that the addition of our anomaly fields will be a minor contribution to the dynamical inconsistencies already present in the CORE forcing fields (Large and Yeager, 2004). The basis of this data is monthly climatological PMIP3 output. Any variables presented on sub-monthly time resolution are therefore time-interpolated. Since this is a limitation of the available data, we have to assume that any sub-monthly variability (e.g. the diurnal cycle) is preserved from the preindustrial climate state to the LGM state. The anomalies are calculated as the mean of the difference between monthly climatologies of the 'lgm' and 'piControl' PMIP3 model runs ~~(denoted LGM and PI hereafter)~~. The calculation of such a model mean will dampen uncorrelated variability across the different models. However, for the sake of achieving long integration times (e.g., for paleo studies), we expect this approach is justifiable. Moreover, the calculated anomalies are generally small as compared to the forcing field itself. In cases where modelling groups provided more than one ensemble member, we included only the first member in our calculations. Even though PMIP3 simulations have limitations and a large inter-model spread, PMIP3 is the state of the art for modelling of past climates at present (Braconnot et al., 2012; Braconnot and Kageyama, 2015). Furthermore, no global proxy-based reconstructions of the variables presented here are available to provide a proxy-based LGM forcing dataset. Using mean coupled model output as forcing is thus considered the best available option for use in forced ocean models. The data is the mean anomaly of ~~four~~ five PMIP3 models (CNRM-CM5, IPSL-CM5A-LR, GISS-E2-R, MIROC-ESM and MRI-CGCM3~~;~~, Table 2), as only these models provide output for all variables.

The variables are i) specific humidity at 10 meters, ii) downwelling longwave radiation, iii) downwelling shortwave radiation, iv) precipitation, v) wind (v and u components), vi) temperature at 10 meters, and vii) sea surface salinity (SSS) (Table 1). The SSS anomaly field can be used to apply SSS restoring in LGM simulations. All variables (Sect. 3.1-7) of the monthly climatological PMIP3 output have been regridded (Table 3, #1), averaged (Table 3, #2), and differenced (Table 3, #3) to calculate the anomaly fields. ~~Changes in the order of the operations leads to differences in the order of round off errors only.~~ Additional procedures for each variable ~~is given~~are provided in the respective part of Sect. 3, together with a figure of each variable's yearly mean anomaly and model spread. Alongside the lgm-piControl anomaly for each variable, the model spread across all five models is made available. This inter-model disagreement is described for each variable in Sect. 3, and could for example be used to guide adjustments of the amplitude of the forcing anomaly for model tuning purposes. Additionally, proxy-base reconstructions are available for some of the variables (e.g., temperature), which can constrain potential adjustments to the forcing anomaly fields. We leave it to the individual modelling groups to make such adjustments to their forcing fields.

All operations were performed with NetCDF toolkits~~either~~ CDO version 1.9.3~~7.0~~ (Schulzweida, 2019) or NCO version 4.6.9. The ~~M~~main functions used are documented in Table 3, and referred to in the text at the first occurrence. The atmospheric anomaly data are on a Gaussian grid, with 192×94 (lon×lat) grid-points. The SSS fields is on a regular 360×180 (lon×lat) grid. Regridding any of the files to a different model grid should be straightforward (e.g., Table 3, #1), as it was ensured that all files contain the information needed for re-gridding. The variables, grid and time resolution are chosen to be compatible with the CORE forcing fields (Large and Yeager, 2004), which have been extensively used in the ocean modelling community (e.g. Griffies et al. (2009); Schwinger et al. (2016)). We anticipate that the variables selected here should be useful in different model set-ups as well. We intend to provide a data set that is flexible with respect to the use of different land-ocean masks in

different models. Therefore, we account for changes in sea-level (i.e. a larger land area in the LGM), which can affect variables in coastline areas, by applying the following masking procedure: i) masking the multi-model mean anomaly with the maximum lgm land mask across all models, then ii) extrapolating the variable over land using a distance-weighted average (Table 3, #4), and iii) finally masking the data with a present-day land mask (based on the World Ocean Atlas 2013 1° resolution land mask), but with the ocean extended in a 1.5 degrees radius over land. This choice ensures that the anomaly forcing data can be used with any pre-industrial land-sea mask. Through following this procedure, the grid points affected by land-sea mask changes are thus filled with the extrapolated model mean anomaly from the LGM coastaln ocean. In the case of NorESM-OC (Schwinger et al., 2016), the atmospheric anomaly fields were added to its CORE normal-year forcing fields (Large and Yeager, 2004) to obtain a LGM normal-year forcing, under the assumption of an unchanged spatial and temporal variability for the respective variable. Note that the addition of the anomaly fields to the user's own model forcing could lead to physically unrealistic/not-meaningful results for some variables (such as negative precipitation or radiation). This must be corrected for by capping off sub-zero values (Table 3, #54) after addition of the anomaly.

3 The variables

3.1 Specific humidity anomaly

The monthly climatology of near-surface specific humidity is provided at 2 meters height in PMIP3. The bulk forcing method of Large and Yeager (2004) requires specific humidity (and temperature) at the same height as the wind forcing (10 meters). Therefore, specific humidity was re-referenced to 10 meters height for each of the four models following the procedure detailed in Large and Yeager (2004). The re-referencing required the use of wind (u and v components), sea level pressure (CMIP variable 'psl') and skin temperature ('ts', representing sea surface temperature over the open ocean), which were taken from the respective 'piControl' and 'lgm' CMIP5/~~PI and LGM~~ PMIP3 output for each model. The mean anomaly over the four models was time interpolated (Table 3, #65) to a 6-hour time resolution from the monthly climatological PMIP3 output. The annual mean lgm-piControl ~~LGM-PI~~ anomaly field (Fig. 1) shows a global decrease in specific humidity, as expected from decreased air temperatures (Sect. 3.6). The anomaly is most pronounced around the equator, where we see a decrease of 2-3 kg kg^{-1}, while the anomaly is near-zero towards both poles. The model spread of the anomaly shows a disagreement between the PMIP3 models generally in the order of 1-2 kg kg^{-1}, without any strong spatial pattern (Fig. 1).

3.2 Downwelling longwave radiation anomaly

The anomaly for surface downwelling longwave radiation is time-interpolated (Table 3, #56) to a daily time resolution. The annual mean anomaly field (Fig. 2) shows globally decreased downwelling longwave radiation in the 'lgm' experiment ~~LGM~~ as compared to the 'piControl' experiment~~PI~~, in the order of 10-30 W m^{-2} over most of the ocean due to a generally cooler atmosphere (Sect. 3.6). The largest anomalies lie close to~~at~~ the northern ice sheets, with up to -90 W m^{-2} lower radiation in the 'lgm' experiment ~~LGM~~ than in the 'piControl' experiment~~PI~~. ~~In addition to influencing radiative forcing over land, i~~Ice is likely also the main contributor to the high (60-90 W m^{-2}) inter-model spread in North Atlantic and Southern Oceans. The remainder of the ocean exhibits a better agreement, with inter-model spreads generally below 20 W m^{-2} (Fig. 2).

3.3 Downwelling shortwave radiation anomaly

The surface downwelling shortwave radiation anomaly field is time-interpolated (Table 3, #6~~5~~) to daily fields as done for downwelling longwave radiation. The annual mean anomaly is especially pronounced around the Laurentide and Scandinavian ice sheets, where strong positive anomalies of over ~30 W m^{-2} exist (Fig. 3). Globally, the annual mean downwelling shortwave radiation anomaly generally falls in a range of -15 to +15 W m^{-2} over the ocean. The anomaly field shows negative anomalies as well positive ones in an alternating spatial pattern approximately symmetrically around the equator in the Pacific basin. The inter-model spread is largest in the North Atlantic region and along the equator (Fig. 3). Due to the large model disagreement of up to 50 W m^{-2} for this variable, the inter-model spread and mean anomaly are of similar magnitude although a consistent pattern is present in the anomaly field.

3.4 Precipitation anomaly

The anomaly presented here is the lgm-piControl~~LGM-PI~~ precipitation anomaly at the air-sea interface and includes both the liquid and solid phases from all types of clouds (both large-scale and convective), and excludes evaporation. The units were converted to mm day^{-1} to comply with the CORE forcing format (causing a deviation from the CF-1.6 convention). The resulting annual mean anomaly generally falls in the range of -2 to 2 mm day^{-1}, and is most pronounced along the equator ~~and in the Northern Hemisphere~~ (Fig. 4). The models show a mean increase in precipitation directly south of the equator in the Pacific basin, as well as in the Pacific subtropics off the western North-American coast. The North Atlantic also receives a mean positive precipitation anomaly, offsetting part of the positive salinity anomaly there, which is potentially relevant for the simulation of deep water formation in this region (Sect. 3.7). Negative mean precipitation anomalies are most pronounced directly north of the equator and north of ~40° N in the Pacific basin as well as in the Atlantic Arctic. The inter-model spread is up to ~5 mm day^{-1} around the equator, likely due to the model disagreement about the sign and location of changes in the inter-tropical convergence zone (Fig. 4). Related to precipitation fluxes, river runoff fluxes also changed between the lgm and piControl model experiments. As river routing and flux calculations are very model specific, we expect modelling groups to find a suitable solution for their setup themselves, and recommend consulting the PMIP guidelines when doing so (Kageyama et al., 2017).

3.5 Wind anomalies, u and v components

Both for the u and v component of the wind speed, the lgm-piControl ~~LGM-PI~~ anomaly is time-interpolated to 6-hourly fields. The annual mean meridional wind velocity (v, southerly winds) anomaly shows a pronounced increase (~3-5 m s^{-1}) in southerly winds around the NW edge of the Laurentide ice sheet as well as over the NW edge of the Scandinavian ice sheet (Fig. 5). Alongside that, a pronounced decrease (~ 3-5 m s^{-1}) in southerly winds is simulated ~~above the Laurentide ice sheet and east of Scandinavia~~along the eastern North American coast and the Canadian archipelago. The open ocean anomalies are generally small (at most ±1 m s^{-1}). The inter-model spread has no pronounced pattern but is sizable, with ~ 1-5 m s^{-1} disagreement between the PMIP3 models. The mean zonal wind velocity (u, westerly winds) anomaly shows alternating negative and positive anomaly bands with an approximate ±2 m s^{-1} range (Fig. 6). This pattern is stronger in the Northern Hemisphere north of ~45° N~~, where ~5 m s^{-1} anomalies exist over the American continent and the North Atlantic ocean basin~~. The inter-model spread

(~1-3 m s^{-1}) has little structure except for the ~4-5 m s^{-1} disagreement in the Southern Ocean south of ~40° S, and the ~3-5 m s^{-1} disagreement in the North Atlantic (Fig. 6).

3.6 Temperature anomaly

The near-surface atmospheric temperature at 2 m height from PMIP3 is re-referenced to 10 meters (as done for specific humidity, Sect. 3.1), and time-interpolated to calculate the 6-hourly mean anomaly for temperature. ~~In order to account for differences in temperature to changes in topography in each of the models, a correction is made for the adiabatic lapse rate. The temperature effect in topography above 10 m is calculated per model using an adiabatic lapse rate effect of 5 degrees per kilometre. The dataset presented here is thus representative of the fictitious temperature at 10 meter above sea level, and should be corrected for the adiabatic lapse rate if applied at a different height (i.e. on land). For flexibility of use, both the topography uncorrected ('tas') and topography corrected ('tas_10m') temperature anomaly data are provided in the netCDF file.~~ The annual mean anomaly is most pronounced in the North Atlantic, where open ocean anomalies exceed 10 K.~~The topography corrected annual mean temperature anomaly is generally negative (~ -3 K), but has extremes around the North Atlantic of around -15 K (Fig. 7).~~ Elsewhere, the annual mean temperature generally is around 2.5 K. There is a clear pattern in the model spread: The models show a large spread (>10 K) ~~over the continents~~ north of ~45° N, as well as south of ~40° S (5-10 K), likely due to the disagreement about ice cover. At lower latitudes and over the ocean the model spread is generally smaller (0-3 K~~), with the only exceptions in the Southern Ocean (5-10 K) and in the North Atlantic (>10 K)~~ (Fig. 7).

3.7 Sea surface salinity anomaly

Global mean salinity is initialized in PMIP3 models with a 1 psu higher salinity to account for the concentrating effect of the decrease in sea level (Kageyama et al., 2017). Sea surface salinity however, shows a more variable annual mean lgm-piControl ~~LGM-PI~~ change due to changes in the global hydrological cycle (Fig. 8). ~~Only the models CNRM-CM5 and MIROC-ESM are used here for the averaging because of data availability. The difference in land-sea mask between the LGM and PI simulations is accounted for by filling any missing values with a distance-weighted mean based on the four nearest neighbours per empty grid cell (Table 3, #6). This results in a SSS anomaly field with values in every grid cell (so essentially without a land-sea mask), such that it can be used with any land-sea mask. In addition, t~~The sea surface salinity anomaly is presented on a regular 1x1 grid for ease of use. ~~The land-sea mask correction is only needed for SSS, as all other variables presented in this text are global atmospheric fields. Because the mean anomaly is locally patchy due to the large model spread and extrapolation, we improve the smoothness of the result using 9-point smoothing as a final step (Table 3, #7).~~ The resulting annual mean SSS anomaly (Fig. 8) shows an increase in sea surface salinity (~1 psu) over the Southern Ocean south of ~55° S, as well as in the Arctic (>3 psu) and the Northern Indian Ocean (~1 psu). A ~2 psu anomaly is simulated in the Canadian Archipelago, the Labrador Sea and across the North Atlantic between what is now Canada and Europe (Fig. 8). Freshening is simulated close to some continents, and is especially pronounced around Scandinavia (about -3 psu). Simulated ocean circulation can be very sensitive to fresh water forcing and thus SSS, especially in the North Atlantic (e.g. Rahmstorf (1996), Spence et al. (2008)). Application of SSS restoring using the SSS anomaly field should therefore be done with caution and attention to its effects on the meridional overturning circulation. Tuning of the salinity anomaly in important deep-water formation regions of up to about

±1 psu, such as done by for example Winguth et al. (1999), may be required to obtain a satisfactory circulation field in reasonable agreement with proxy data. Such adjustments fall well within the PMIP3 model spread (Fig. 8), and show the current limitations of fully coupled PMIP3 models to simulate the LGM hydrological cycle consistent with proxy records of ocean circulation.

4 Data availability

The data are publicly accessible at the NIRD Research Data Archive at https://doi.org/10.11582/2019.00019 (Morée and Schwinger, 2019). The .md5 files contain an md5 checksum, which can be used to check whether changes have been made to the respective .nc files. ~~at https://doi.org/10.11582/2019.00011 (Morée and Schwinger, 2019).~~

5 Summary and Conclusions

The output of the fully coupled PMIP3 simulations of CNRM-CM5, IPSL-CM5A-LR, MIROC-ESM and MRI-CGCM3 is converted to anomaly datasets intended for use in forced ocean modelling of the LGM. All anomalies are calculated as the difference between the 'lgm'~~LGM~~ and 'piControl'~~PI~~ PMIP3 experiments. In addition, all data are formatted in a way that further conversions (of for example units or the grid) can be applied in a straightforward way. The variables are provided in ~~netCDF~~ NetCDF format in separate files, and distributed by the NIRD Research Data Archive (Morée and Schwinger, 2019). A climatological LGM forcing data set can be created for any forced ocean model by addition of the presented 2-D anomaly fields to the model's pre-industrial forcing. This approach enables the scientific community to simulate the LGM ocean state in a forced model set-up. We expect that if additional forcing is needed for a specific model, the same approach as described above can be followed. This process is simplified by providing all main CDO and NCO commands used in creating the dataset (Table 3). All data represent a climatological year, i.e. one annual cycle per variable. The application of the data is thus suitable for 'time-slice' equilibrium simulations of the LGM, and optimised for use with the CORE forcing format (Large and Yeager, 2004).

The uncertainty of our anomaly forcing (approximated by the model spread of the PMIP3 models) is generally of similar magnitude as the multi-model annual mean. The attribution of the model spread to specific processes is beyond the scope of this article, but our results show that there is considerable uncertainty involved in the magnitude of the anomaly for all variables presented here. Nevertheless, all mean anomalies show a distinct spatial pattern that we expect to be indicative of the LGM-PI changes. Finally, there is no other way to reconstruct most of these variables than model simulations with state-of-the-art models such as those applied in the PMIP3 experiments. For modelling purposes, the inter-model disagreement of PMIP3 provides the user with leeway to adjust the amplitude of the forcing (guided by the size of the model spread, which is therefore provided alongside the variables in the dataset). Such adjustments can improve model-proxy data agreements, such as described for salinity in Sect. 3.7.

Author contributions. AM prepared, visualized and analysed the data and wrote the original draft of the manuscript. AM and JS together conceptualized the method and revised the manuscript. JS provided supervision throughout the study.

Competing interests. The authors declare that they have no conflict of interest.

Acknowledgements. We acknowledge the World Climate Research Programme's Working Group on Coupled Modelling, which is responsible for CMIP, and we thank the climate modelling groups (Table 2) for producing and making available their model output. For CMIP the U.S. Department of Energy's Program for Climate Model Diagnosis and Intercomparison provides coordinating support and led development of software infrastructure in partnership with the Global Organization for Earth System Science Portals. This is a contribution to the Bjerknes Centre for Climate Research (Bergen, Norway). Storage resources were provided by UNINETT Sigma2 - the National Infrastructure for High Performance Computing and Data Storage in Norway (project number ns2980k). Anne L. Morée is grateful for PhD funding through the Faculty for Mathematics and Natural Sciences of the University of Bergen. Jörg Schwinger acknowledges funding through the Research Council of Norway (project INES (270061)). This study is a contribution to the project "Coordinated Research in Earth Systems and Climate: Experiments, kNowledge, Dissemination and Outreach" (CRESCENDO; EU Horizon2020 Programme grant no. 641816) which is funded by the European Commission.

References

Braconnot, P., Otto-Bliesner, B., Harrison, S., Joussaume, S., Peterchmitt, J. Y., Abe-Ouchi, A., Crucifix, M., Driesschaert, E., Fichefet, T., Hewitt, C. D., Kageyama, M., Kitoh, A., Laîné, A., Loutre, M. F., Marti, O., Merkel, U., Ramstein, G., Valdes, P., Weber, S. L., Yu, Y., and Zhao, Y.: Results of PMIP2 coupled simulations of the Mid-Holocene and Last Glacial Maximum; Part 1: experiments and large-scale features, Clim. Past, 3, 261-277, 10.5194/cp-3-261-2007, 2007.

Braconnot, P., Harrison, S., Kageyama, M., Bartlein, P., Masson-Delmotte, V., Abe-Ouchi, A., Otto-Bliesner, B., and Zhao, Y.: Evaluation of climate models using palaeoclimatic data, Nature Climate Change, 2, 417-424, doi: 10.1038/nclimate1456, 2012.

Braconnot, P., and Kageyama, M.: Shortwave forcing and feedbacks in Last Glacial Maximum and Mid-Holocene PMIP3 simulations, Philosophical Transactions of the Royal Society A: Mathematical, Physical and Engineering Sciences, 373, 20140424, 10.1098/rsta.2014.0424, 2015.

Brady, E. C., Otto-Bliesner, B. L., Kay, J. E., and Rosenbloom, N.: Sensitivity to Glacial Forcing in the CCSM4, Journal of Climate, 26, 1901-1925, 10.1175/JCLI-D-11-00416.1, 2012.

Caubel, A., Denvil, S., Foujols, M. A., Marti, O., Dufresne, J.-L., Bopp, L., Cadule, P., Ethé, C., Idelkadi, A., Mancip, M., Masson, S., Mignot, J., Ionela, M., Balkanski, Y., Bekki, S., Bony, S., Braconnot, P., Brockman, P., Codron, F., Cozic, A., Cugnet, D., Fairhead, L., Fichefet, T., Flavoni, S., Guez, L., Guilyardi, E., Hourdin, F., Ghattas, J., Kageyama, M., Khodri, M., Labetoulle, S., Lefebvre, M.-P., Levy, C., Li, L., Lott, F., Madec, G., Marchand, M., Meurdesoif, Y., Rio, C., Schulz, M., Swingedouw, D., Szopa, S., Viovy, N., and Vuichard, N.: IPSL-CM5A-LR model output prepared for CMIP5 piControl experiment, served by ESGF,WDCC at DKRZ, doi:10.1594/WDCC/CMIP5.IPILpc, 2016.

Dufresne, J. L., Foujols, M. A., Denvil, S., Caubel, A., Marti, O., Aumont, O., Balkanski, Y., Bekki, S., Bellenger, H., Benshila, R., Bony, S., Bopp, L., Braconnot, P., Brockmann, P., Cadule, P., Cheruy, F., Codron, F., Cozic, A., Cugnet, D., de Noblet, N., Duvel, J. P., Ethé, C., Fairhead, L., Fichefet, T., Flavoni, S., Friedlingstein, P., Grandpeix, J. Y., Guez, L., Guilyardi, E., Hauglustaine, D., Hourdin, F., Idelkadi, A., Ghattas, J., Joussaume, S., Kageyama, M., Krinner, G., Labetoulle, S., Lahellec, A., Lefebvre, M. P., Lefevre, F., Levy, C., Li, Z. X., Lloyd, J., Lott, F., Madec, G., Mancip, M., Marchand, M., Masson, S., Meurdesoif, Y., Mignot, J., Musat, I., Parouty, S., Polcher, J., Rio, C., Schulz, M., Swingedouw, D., Szopa, S., Talandier, C., Terray, P., Viovy, N., and Vuichard, N.: Climate change projections using the IPSL-CM5 Earth System Model: from CMIP3 to CMIP5, Clim Dyn, 40, 2123-2165, 10.1007/s00382-012-1636-1, 2013.

Eyring, V., Bony, S., Meehl, G. A., Senior, C. A., Stevens, B., Stouffer, R. J., and Taylor, K. E.: Overview of the Coupled Model Intercomparison Project Phase 6 (CMIP6) experimental design and organization, Geosci. Model Dev., 9, 1937-1958, 10.5194/gmd-9-1937-2016, 2016.

Griffies, S. M., Biastoch, A., Böning, C., Bryan, F., Danabasoglu, G., Chassignet, E. P., England, M. H., Gerdes, R., Haak, H., Hallberg, R. W., Hazeleger, W., Jungclaus, J., Large, W. G., Madec, G., Pirani, A., Samuels, B. L., Scheinert, M., Gupta, A. S., Severijns, C. A., Simmons, H. L., Treguier, A. M., Winton, M., Yeager, S., and Yin, J.: Coordinated Ocean-ice Reference Experiments (COREs), Ocean Modelling, 26, 1-46, https://doi.org/10.1016/j.ocemod.2008.08.007, 2009.

JAMSTEC, AORI, and NIES: MIROC-ESM model output prepared for CMIP5 piControl, served by ESGF, doi:10.1594/WDCC/CMIP5.MIMEpc 2015a.

JAMSTEC, AORI, and NIES: MIROC-ESM model output prepared for CMIP5 lgm, served by ESGF, doi:10.1594/WDCC/CMIP5.MIMElg, 2015b.

Kageyama, M., Denvil, S., Foujols, M. A., Caubel, A., Marti, O., Dufresne, J.-L., Bopp, L., Cadule, P., Ethé, C., Idelkadi, A., Mancip, M., Masson, S., Mignot, J., Ionela, M., Balkanski, Y., Bekki, S., Bony, S., Braconnot, P., Brockman, P., Codron, F., Cozic, A., Cugnet, D., Fairhead, L., Fichefet, T., Flavoni, S., Guez, L., Guilyardi, E., Hourdin, F., Ghattas, J., Khodri, M., Labetoulle, S., Lefebvre, M.-P., Levy, C., Li, L., Lott, F., Madec, G., Marchand, M., Meurdesoif, Y., Rio, C., Schulz, M., Swingedouw, D., Szopa, S., Viovy, N., and Vuichard, N.: IPSL-CM5A-LR model output prepared for CMIP5 lgm experiment, served by ESGF,WDCC at DKRZ doi:10.1594/WDCC/CMIP5.IPILlg, 2016.

Kageyama, M., Albani, S., Braconnot, P., Harrison, S. P., Hopcroft, P. O., Ivanovic, R. F., Lambert, F., Marti, O., Peltier, W. R., Peterschmitt, J. Y., Roche, D. M., Tarasov, L., Zhang, X., Brady, E. C., Haywood, A. M., LeGrande, A. N., Lunt, D. J., Mahowald, N. M., Mikolajewicz, U., Nisancioglu, K. H., Otto-Bliesner, B. L., Renssen, H., Tomas, R. A., Zhang, Q., Abe-Ouchi, A., Bartlein, P. J., Cao, J., Li, Q., Lohmann, G., Ohgaito, R., Shi, X., Volodin, E., Yoshida, K., Zhang, X., and Zheng, W.: The PMIP4 contribution to CMIP6 – Part 4: Scientific objectives and experimental design of the PMIP4-CMIP6 Last Glacial Maximum experiments and PMIP4 sensitivity experiments, Geosci. Model Dev., 10, 4035-4055, 10.5194/gmd-10-4035-2017, 2017.

Kageyama, M., Braconnot, P., Harrison, S. P., Haywood, A. M., Jungclaus, J. H., Otto-Bliesner, B. L., Peterschmitt, J. Y., Abe-Ouchi, A., Albani, S., Bartlein, P. J., Brierley, C., Crucifix, M., Dolan, A., Fernandez-Donado, L., Fischer, H., Hopcroft, P. O., Ivanovic, R. F., Lambert, F., Lunt, D. J., Mahowald, N. M., Peltier, W. R., Phipps, S. J., Roche, D. M., Schmidt, G. A., Tarasov, L., Valdes, P. J., Zhang, Q., and Zhou, T.: The PMIP4 contribution to CMIP6 – Part 1: Overview and over-arching analysis plan, Geosci. Model Dev., 11, 1033-1057, 10.5194/gmd-11-1033-2018, 2018.

Large, W. G., and Yeager, S. G.: Diurnal to decadal global forcing for ocean and sea-ice models: the data sets and flux climatologies, Tech. Note NCAR/TN-460+STR. National Center of Atmospheric Research, Boulder, Colorado, USA, http://opensky.ucar.edu/islandora/object/technotes:434, 2004.

Marzocchi, A., and Jansen, M. F.: Connecting Antarctic sea ice to deep-ocean circulation in modern and glacial climate simulations, Geophysical Research Letters, 44, 6286-6295, 10.1002/2017GL073936, 2017.

Menviel, L., Yu, J., Joos, F., Mouchet, A., Meissner, K. J., and England, M. H.: Poorly ventilated deep ocean at the Last Glacial Maximum inferred from carbon isotopes: A data-model comparison study, Paleoceanography, 32, 2-17, 10.1002/2016pa003024, 2017.

Morée, A., Schwinger, J.: PMIP3-based Last Glacial Maximum (LGM) pre-industrial (PI) anomaly fields for addition to PI ocean model forcing, version 2~~Last Glacial Maximum minus pre-industrial anomaly fields for use in forced ocean modelling, based on PMIP3~~, Norstore, https://doi.org/10.11582/2019.0001~~9~~1, 2019.

Muglia, J., and Schmittner, A.: Glacial Atlantic overturning increased by wind stress in climate models, Geophysical Research Letters, 42, 9862-9868, doi:10.1002/2015gl064583, 2015.

NASA-GISS: GISS-E2-R model output prepared for CMIP5 pre-industrial control, served by ESGF WDCC at DKRZ, doi:10.1594/WDCC/CMIP5.GIGRpc, 2014a.

NASA-GISS: GISS-E2-R model output prepared for CMIP5 last glacial maximum, served by ESGF WDCC at DKRZ, doi:10.1594/WDCC/CMIP5.GIGRlg, 2014b.

Otto-Bliesner, B. L., Hewitt, C. D., Marchitto, T. M., Brady, E., Abe-Ouchi, A., Crucifix, M., Murakami, S., and Weber, S. L.: Last Glacial Maximum ocean thermohaline circulation: PMIP2 model intercomparisons and data constraints, Geophysical Research Letters, 34, 10.1029/2007GL029475, 2007.

Rahmstorf, S.: On the freshwater forcing and transport of the Atlantic thermohaline circulation, Clim Dyn, 12, 799-811, 10.1007/s003820050144, 1996.

Schmidt, G. A., Kelley, M., Nazarenko, L., Ruedy, R., Russell, G. L., Aleinov, I., Bauer, M., Bauer, S. E., Bhat, M. K., Bleck, R., Canuto, V., Chen, Y.-H., Cheng, Y., Clune, T. L., Del Genio, A., de Fainchtein, R., Faluvegi, G., Hansen, J. E., Healy, R. J., Kiang, N. Y., Koch, D., Lacis, A. A., LeGrande, A. N., Lerner, J., Lo, K. K., Matthews, E. E., Menon, S., Miller, R. L., Oinas, V., Oloso, A. O., Perlwitz, J. P., Puma, M. J., Putman, W. M., Rind, D., Romanou, A., Sato, M., Shindell, D. T., Sun, S., Syed, R. A., Tausnev, N., Tsigaridis, K., Unger, N.,

Voulgarakis, A., Yao, M.-S., and Zhang, J.: Configuration and assessment of the GISS ModelE2 contributions to the CMIP5 archive, Journal of Advances in Modeling Earth Systems, 6, 141-184, 10.1002/2013MS000265, 2014.

Schulzweida, U.: CDO User Guide (Version 1.9.6), Max Planck Institute for Meteorology, Bundesstraße 53, 20146 Hamburg, Germany, http://doi.org/10.5281/zenodo.2558193, 215 pp., 2019.

Schwinger, J., Goris, N., Tjiputra, J. F., Kriest, I., Bentsen, M., Bethke, I., Ilicak, M., Assmann, K. M., and Heinze, C.: Evaluation of NorESM-OC (versions 1 and 1.2), the ocean carbon-cycle stand-alone configuration of the Norwegian Earth System Model (NorESM1), Geosci. Model Dev., 9, 2589-2622, 10.5194/gmd-9-2589-2016, 2016.

Sénési, S., Richon, J., Franchistéguy, L., Tyteca, S., Moine, M.-P., Voldoire, A., Sanchez-Gomez, E., Salas y Mélia, D., Decharme, B., Cassou, C., Valcke, S., Beau, I., Alias, A., Chevallier, M., Déqué, M., Deshayes, J., Douville, H., Madec, G., Maisonnave, E., Planton, S., Saint-Martin, D., Szopa, S., Alkama, R., Belamari, S., Braun, A., Coquart, L., and Chauvin, F.: CNRM-CM5 model output prepared for CMIP5 piControl, served by ESGF,WDCC at DKRZ, doi:10.1594/WDCC/CMIP5.CEC5pc, 2014a.

Sénési, S., Richon, J., Franchistéguy, L., Tyteca, S., Moine, M.-P., Voldoire, A., Sanchez-Gomez, E., Salas y Mélia, D., Decharme, B., Cassou, C., Valcke, S., Beau, I., Alias, A., Chevallier, M., Déqué, M., Deshayes, J., Douville, H., Madec, G., Maisonnave, E., Planton, S., Saint-Martin, D., Szopa, S., Alkama, R., Belamari, S., Braun, A., Coquart, L., and Chauvin, F.: CNRM-CM5 model output prepared for CMIP5 lgm, served by ESGF,WDCC at DKRZ, doi:10.1594/WDCC/CMIP5.CEC5lg, 2014b.

Spence, J. P., Eby, M., and Weaver, A. J.: The Sensitivity of the Atlantic Meridional Overturning Circulation to Freshwater Forcing at Eddy-Permitting Resolutions, Journal of Climate, 21, 2697-2710, 10.1175/2007JCLI2103.1, 2008.

Sueyoshi, T., Ohgaito, R., Yamamoto, A., Chikamoto, M. O., Hajima, T., Okajima, H., Yoshimori, M., Abe, M., O'Ishi, R., Saito, F., Watanabe, S., Kawamiya, M., and Abe-Ouchi, A.: Set-up of the PMIP3 paleoclimate experiments conducted using an Earth system model, MIROC-ESM, Geosci. Model Dev., 6, 819-836, 10.5194/gmd-6-819-2013, 2013.

Taylor, K. E., Stouffer, R. J., and Meehl, G. A.: An Overview of CMIP5 and the Experiment Design, Bulletin of the American Meteorological Society, 93, 485-498, 10.1175/BAMS-D-11-00094.1, 2011.

Voldoire, A., Sanchez-Gomez, E., Salas y Mélia, D., Decharme, B., Cassou, C., Sénési, S., Valcke, S., Beau, I., Alias, A., Chevallier, M., Déqué, M., Deshayes, J., Douville, H., Fernandez, E., Madec, G., Maisonnave, E., Moine, M. P., Planton, S., Saint-Martin, D., Szopa, S., Tyteca, S., Alkama, R., Belamari, S., Braun, A., Coquart, L., and Chauvin, F.: The CNRM-CM5.1 global climate model: description and basic evaluation, Clim Dyn, 40, 2091-2121, 10.1007/s00382-011-1259-y, 2013.

Winguth, A. M. E., Archer, D., Duplessy, J. C., Maier-Reimer, E., and Mikolajewicz, U.: Sensitivity of paleonutrient tracer distributions and deep-sea circulation to glacial boundary conditions, Paleoceanography, 14, 304-323, 10.1029/1999PA900002, 1999.

Yukimoto, S., Adachi, Y., Hosaka, M., Sakami, T., Yoshimura, H., Hirabara, M., Tanaka, T. Y., Shindo, E., Tsujino, H., Deushi, M., Mizuta, R., Yabu, S., Obata, A., Nakano, H., Koshiro, T., Ose, T., and Kitoh, A.: A New Global Climate Model of the Meteorological Research Institute: MRI-CGCM3;Model Description and Basic Performance, Journal of the Meteorological Society of Japan. Ser. II, 90A, 23-64, 10.2151/jmsj.2012-A02, 2012.

Yukimoto, S., Adachi, Y., Hosaka, M., Sakami, T., Yoshimura, H., Hirabara, M., Tanaka, T., Shindo, E., Tsujino, H., Deushi, M., Mizuta, R., Yabu, S., Obata, A., Nakano, H., Koshiro, T., Ose, T., and Kitoh, A.: MRI-CGCM3 model output prepared for CMIP5 piControl, served by ESGF,WDCC at DKRZ, doi:10.1594/WDCC/CMIP5.MRMCpc, 2015a.

Yukimoto, S., Adachi, Y., Hosaka, M., Sakami, T., Yoshimura, H., Hirabara, M., Tanaka, T., Shindo, E., Tsujino, H., Deushi, M., Mizuta, R., Yabu, S., Obata, A., Nakano, H., Koshiro, T., Ose, T., and Kitoh, A.: MRI-CGCM3 model output prepared for CMIP5 lgm, served by ESGF,WDCC at DKRZ, doi:10.1594/WDCC/CMIP5.MRMClg, 2015b.

Variable description	Units	Resolution (lon×lat), time	Notes	Variable name~~(s)~~	PMIP3 variable name(s)
Specific humidity	kg kg^{-1}	192×94, 1460	Re-referenced to 10 m	huss_10m	huss
Downwelling longwave radiation	W m^{-2}	192×94, 365		rlds	rlds
Downwelling shortwave radiation	W m^{-2}	192×94, 365		rsds	rsds
Precipitation	mm day^{-1}	192×94, 12		pr	pr
Wind (u and v components)	m s^{-1}	192×94, 1460		uas and vas	uas and vas
Temperature	K	192×94, 1460	Re-referenced to 10 m	~~tas (re-referenced)~~ tas_10m ~~(re-referenced and topography corrected)~~ ~~tas_diff (= tas - tas_10m = temperature effect)~~	tas
Sea surface salinity	psu	360×180, 12	~~CNRM-CM5 and MIROC-ESM only~~	sos	so~~s~~

Table 1: Summary of the data showing variable description, units, format (lon×lat, time), Notes, N~~n~~etCDF variable name(s) and the original PMIP3 variable name(s). Formats follow CORE conventions (Large and Yeager, 2004). The wind component variables are provided in separate files (Morée and Schwinger, 2019). In each NetCDF file (i.e., for each variable) the model spread is provided alongside the anomaly field named 'variablename_spread'.

Model name	Modelling group	Reference	Source data reference
CNRM-CM5	CNRM-CERFACS (France)	Voldoire et al. (2013)	piControl: Sénési et al. (2014a) lgm: Sénési et al. (2014b)
IPSL-CM5A-LR	IPSL (Institut Pierre Simon Laplace, France)	Dufresne et al. (2013)	piControl: Caubel et al. (2016) lgm: Kageyama et al. (2016)
MIROC-ESM	MIROC (JAMSTEC and NIES, Japan)	Sueyoshi et al. (2013)	piControl: JAMSTEC et al. (2015a) lgm: JAMSTEC et al. (2015b)
MRI-CGCM3	MRI (Meteorological Research Institute, Japan)	Yukimoto et al. (2012)	piControl: Yukimoto et al. (2015a) lgm: Yukimoto et al. (2015b)
GISS-E2-R	NASA/GISS (Goddard Institute for Space Studies, USA)	Schmidt et al. (2014)	piControl: NASA-GISS (2014a) lgm: NASA-GISS (2014b)

Table 2: PMIP3 models used in this study

#	CDO or NCO command
1	cdo remapbil,t62grid
2	cdo ensmean~~ncea~~
3	cdo sub~~ncdiff~~
4	cdo setmisstodis~~ncap2~~
5	ncap2~~cdo inttime~~
6	cdo inttime~~cdo setmisstodis~~
~~7~~	~~cdo smooth9~~

Table 3: Package commands applied in this study. Detailed information on these commands can be found in the respective NCO and CDO documentation online. All operations were performed with either CDO version 1.9.3~~7.0~~ (Schulzweida, 2019) or NCO version 4.6.9. The complete list of commands is available in the NetCDF files as global attribute 'history'.

5

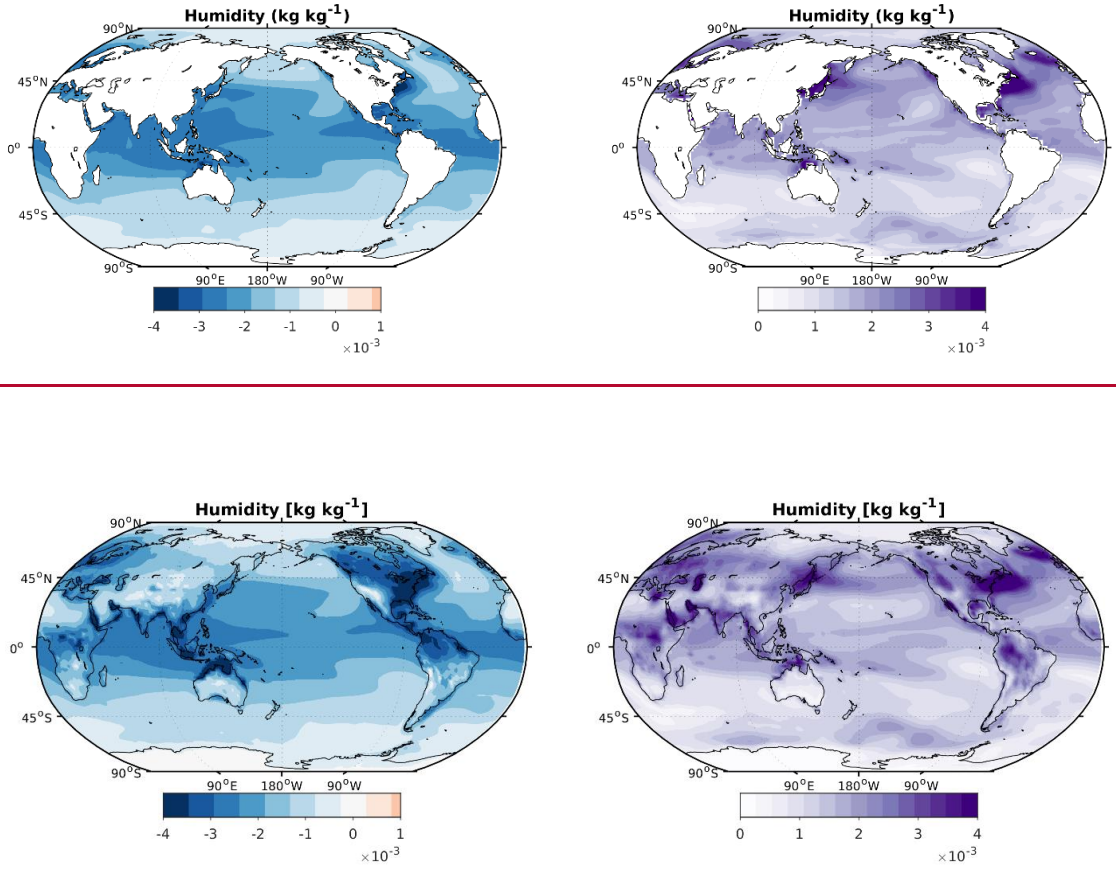

Figure 1: Annual mean 10-meter height specific humidity lgm-piControl ~~LGM-PI~~ anomaly (left) and model spread (right) in kg kg^{-1}.

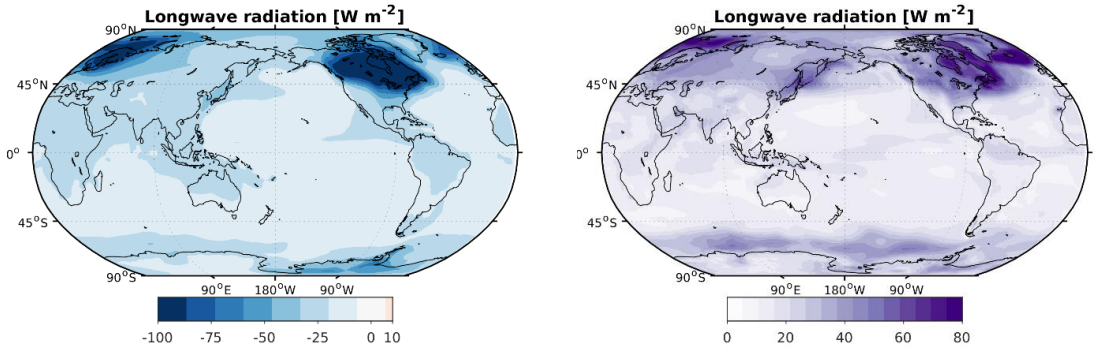

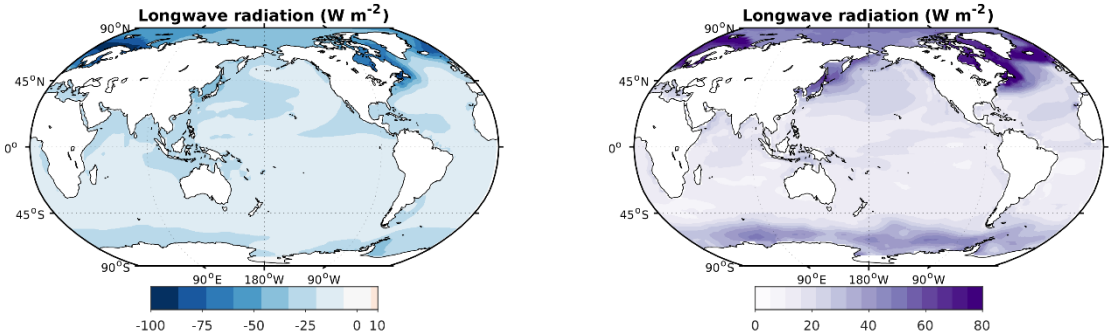

Figure 2: Annual mean downwelling longwave radiation lgm-piControl~~LGM-PI~~ anomaly (left) and model spread (right) in W m^{-2}.

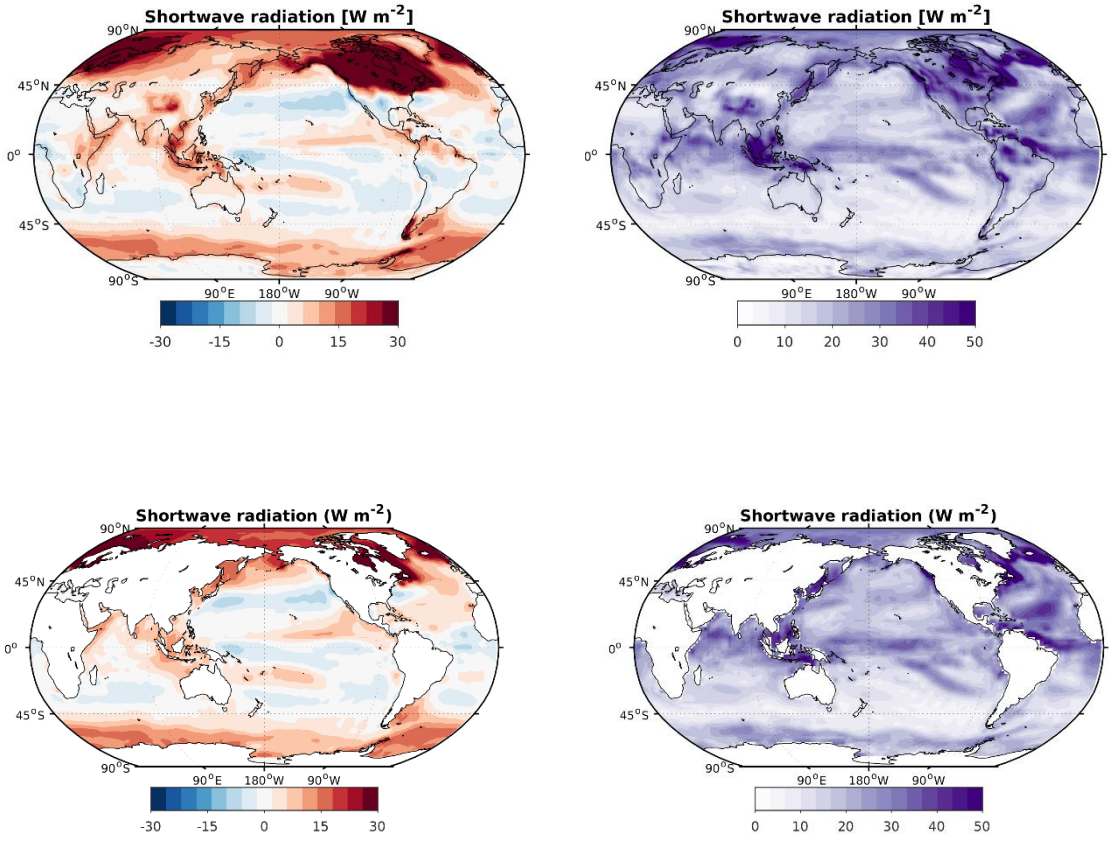

Figure 3: Annual mean downwelling shortwave radiation lgm-piControl~~LGM-PI~~ anomaly (left) and model spread (right) in W m^{-2}.

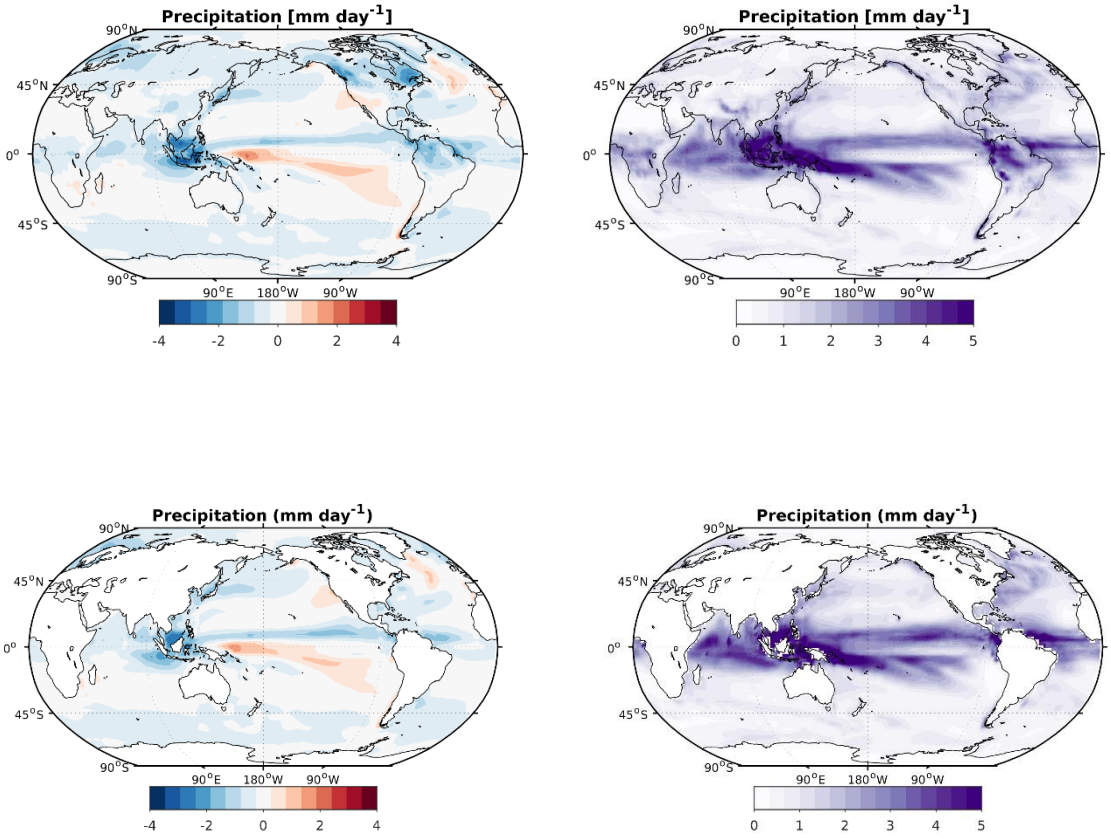

Figure 4: Annual mean precipitation lgm-piControl~~LGM-PI~~ anomaly (left) and model spread (right) in mm day^{-1}.

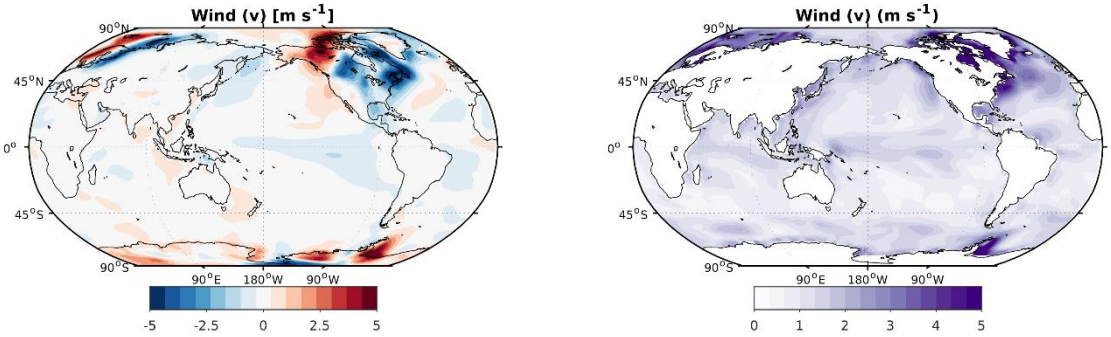

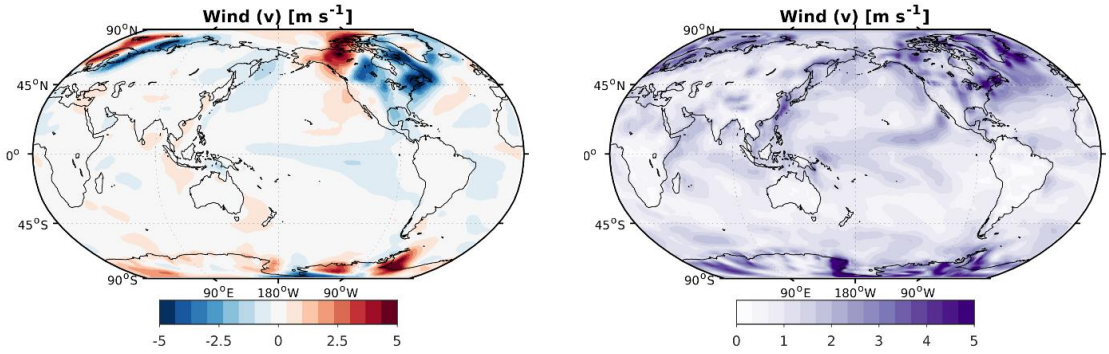

Figure 5: Annual mean meridional wind velocity lgm-piControl~~LGM-PI~~ anomaly (left) and model spread (right) in m s^{-1}.

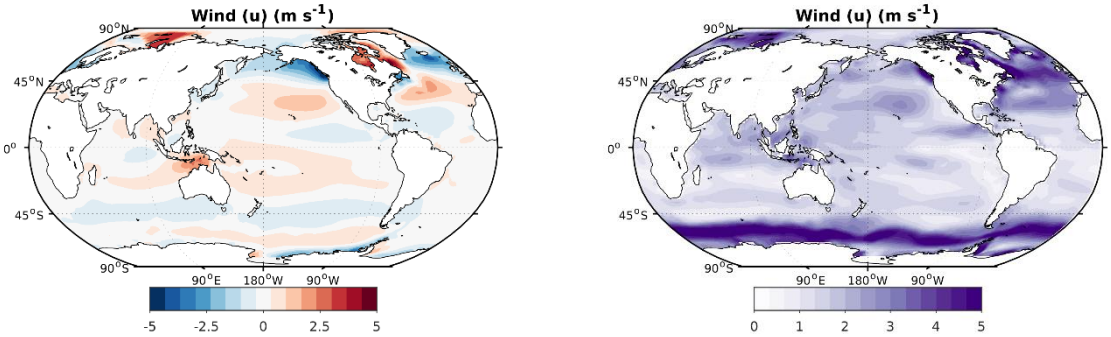

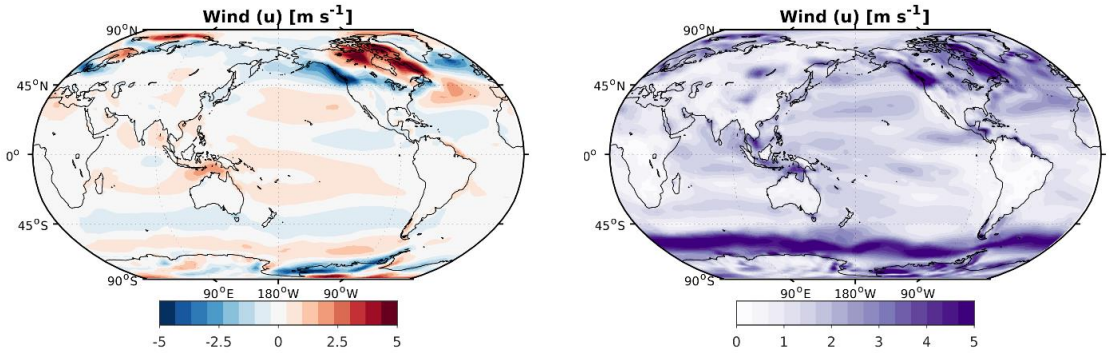

Figure 6: Annual mean zonal wind velocity lgm-piControl~~LGM-PI~~ anomaly (left) and model spread (right) in m s^{-1}.

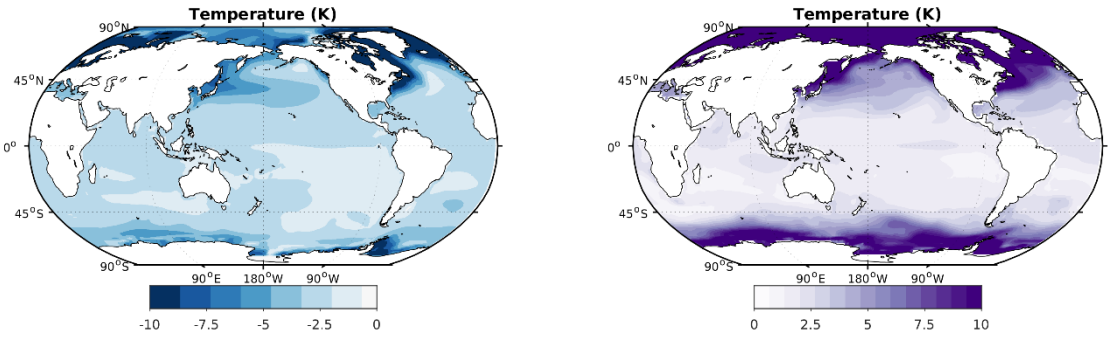

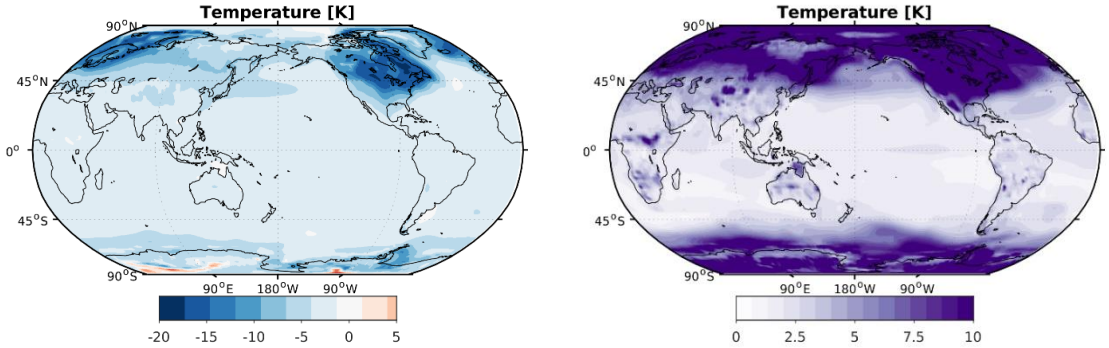

Figure 7: Annual mean ~~topography corrected~~ 10-meter height temperature lgm-piControl~~LGM-PI~~ anomaly (left) and model spread (right) in K.

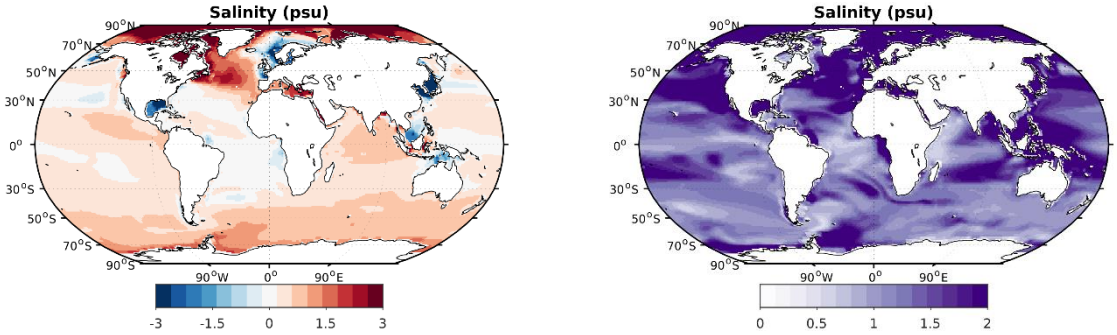

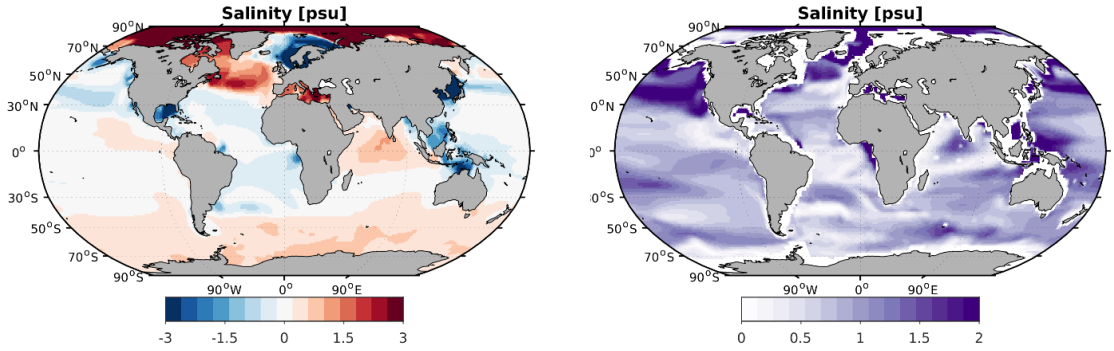

Figure 8: Annual mean sea surface salinity lgm-piControl~~LGM-PI~~ anomaly (left) and model spread (right) in psu.